PROCEEDINGS OF SCIENCE

Mid-infrared properties of local active galactic nuclei at high angular resolution

Daniel Asmus*
Max-Planck-Institut für Radioastronomie, Auf dem Hügel 69, 53121 Bonn, Germany
E-mail: asmus@mpifr.de

Poshak Gandhi
Institute of Space and Astronautical Science (ISAS), Japan Aerospace Exploration Agency, 3-1-1 Yoshinodai, chuo-ku, Sagamihara, Kanagawa 252-5210, Japan

Sebastian F. Hönig
UCSB Department of Physics, Broida Hall 93106-9530, Santa Barbara, CA, USA

Alain Smette
European Southern Observatory, Casilla 19001, Santiago 19, Chile

We present the largest mid-infrared atlas of active galactic nuclei at sub-arcsecond spatial scales containing 249 objects. It comprises all ground-based HR MIR observations performed to date. This catalog also includes a large number of new observations. The photometry in multiple filters allows for characterization of the properties of the dust emission for most objects. We derive upper limits on the star formation contribution toward the unresolved nuclear emission and assess whether the AGN dominates the MIR emission of the galaxies. Furthermore, the AGN MIR atlas is well-suited for AGN unification studies because of its size and characteristics. We discuss the enlarged MIR–X-ray correlation, which extends over six orders of magnitude in luminosity and potentially probes different physical mechanisms, as an example.

Nuclei of Seyfert galaxies and QSOs - Central engine & conditions of star formation,
November 6-8, 2012
Max-Planck-Insitut für Radioastronomie (MPIfR), Bonn, Germany

*Speaker.

PoS(Seyfert 2012)007

1. Introduction

Mid-infrared (MIR) observations enable the study of the astrophysical dust in active galactic nuclei (AGN). This dust plays a key role in our understanding of the central accreting supermassive black hole and the surrounding star formation (SF). During the last decade, an increasing number of articles have demonstrated the power and importance of high-angular resolution (HR) MIR observations in order to isolate the AGN from surrounding starbursts, e.g., [6, 4, 12, 1]. However, owing to the comparably low sensitivity and higher complexity of ground-based MIR observations (contrary to low-angular resolution space-based with, e.g., *Spitzer*), only relatively small samples have been observed and analyzed so far.

While HR enables us to resolve non-AGN emission regions in the nuclear regions of nearby galaxies, the AGN itself remains mostly unresolved even with 8 meter class telescopes (apart from the outer narrow line region). Many components of the AGN can possibly emit significant MIR emission, including the accretion disk surrounding the central supermassive black hole (SMBH), the perpendicularly emitted highly beamed jet outflow, the emission line clouds and the dusty obscuring structure ('torus') .

Finally, MIR interferometric observations enable us to resolve the AGN components but due to the sensitivity limits, only a relatively small number of AGN can be studied.

For these reasons, this project aims top provide an understanding of the MIR emitting structure in AGN by assembling HR MIR spectral energy distributions for a large representative sample of local AGN. This can then be used for multiwavelength studies as presented here, in particular the MIR–X-ray relation. The full analysis of this dataset will be published in Asmus et al. (in prep, a,b).

2. Sample selection and observations

High angular resolution is of utmost importance for the study of the MIR properties of local AGN. Therefore, we have considered imaging observations of only the largest single dish facilities in order to amass an AGN atlas of all ground-based MIR observations ever taken. In particular, we concentrate on facilities with public archives: Gemini/Michelle[5], Gemini/T-ReCS[13], Subaru/COMICS[8], and VLT/VISIR[11].

The base sample of this study is the uniform BAT 9-month AGN sample consisting of 104 objects[15]. Of those, we have observed a subsample of 80 sources with at least one of the above instruments during the last few years. Despite its selection method at hardest X-rays (14-195 keV), the BAT AGN sample underrepresents the highest absorbed part of the AGN population, in particular Compton-thick objects. Furthermore, the rather high flux limit leads to a cutoff of most low-luminosity AGN, which represent the majority of the nearby AGN. For these reasons, we have complemented the BAT AGN sample with all local AGN that have imaging observations available in at least one of the four instruments (COMICS, Michelle, T-ReCS and VISIR). In this work, we define 'local' as redshift $z \leq 0.4$. This selection leads to a total sample of 249 AGN with a median redshift of 0.016, the 'AGN MIR atlas'. Note that this atlas is not complete in terms of volume or flux thresholds but simply contains everything that has been observed to date. However, with respect to [14], the AGN MIR atlas contains more than one-third of all optically identified AGN

with a redshift < 0.01. Furthermore, it is sufficiently large to allow construction of well-matched samples based upon various selection strategies in future investigations. In the following of this work, we only distinguish between type 1 (Sy 1.0-1.5, and 1n), and type 2 (Sy 1.8-2.0 and 1h, 1i) AGN and LINERs (low-ionization nuclear emission line regions). With this definition, the majority of the objects are type 2. In total, about 1000 N- and Q-band images have been analyzed, of which more than 600 are yet unpublished. The majority of images have been obtained with VISIR, followed by T-ReCS, Michelle, and the least with COMICS. All observations have been carried out in standard chopping and nodding mode. Usually a flux standard star was observed within the two hours prior to or following the AGN and is used for the flux calibration. The flux measurements are carried out in the same way as described in [1] using a custom Gaussian fitting photometry method.

3. Results

Out of the 249 AGN, 200 have been clearly detected. The majority of images show compact or point-like nuclear emission, and no host galaxy emission is detected (Fig. 1). In total, $\sim 18\%$ of the

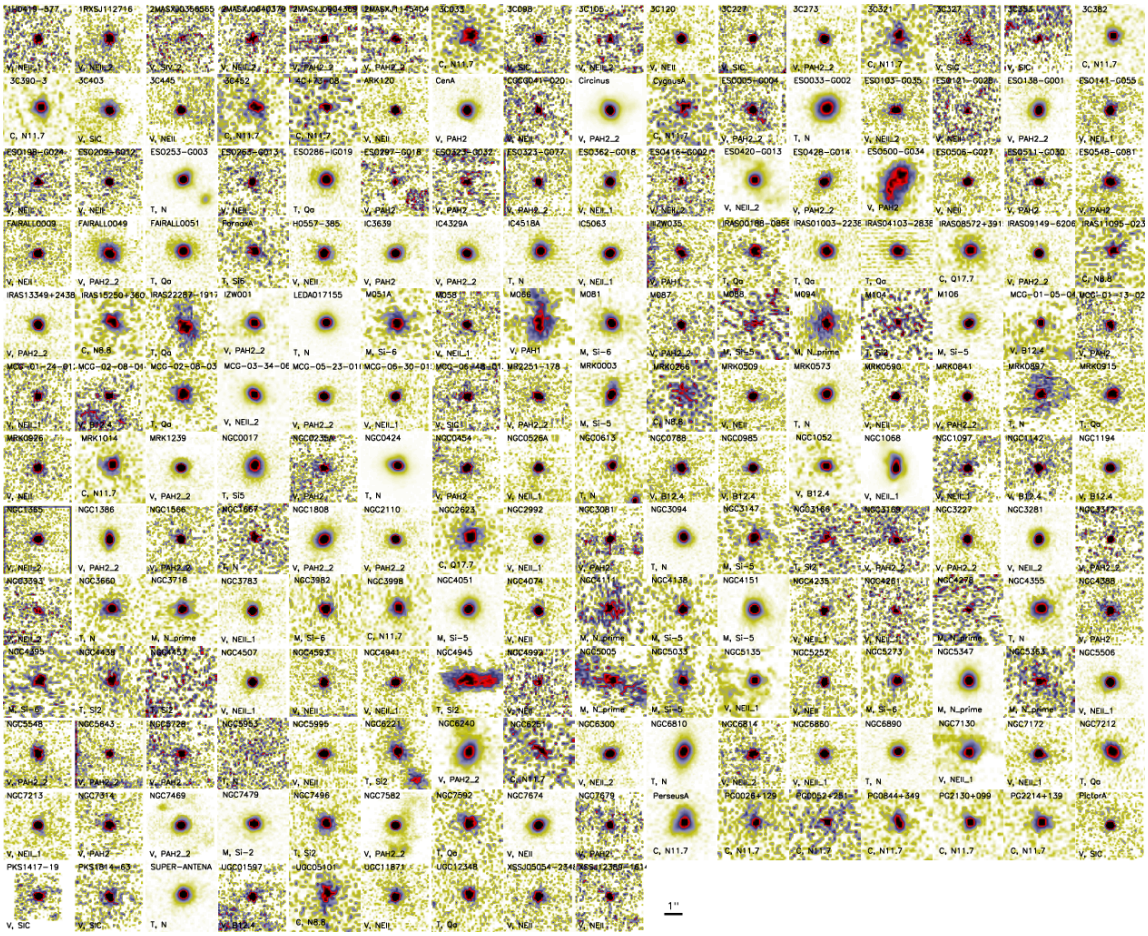

Figure 1: Example MIR images of the inner 4 arcsec of the detected AGN from the atlas (various filters). The color scaling is linear in terms of the standard deviation of the local background, σ_{BG}, while white corresponds to median or below-median background.

objects show consistent evidence of at least partly resolved nuclear or circumnuclear MIR emission. The unresolved nuclear MIR emission measured in all images is used for further analysis in the following. In particular, we concentrate on the MIR emission at $\sim 12\,\mu$m measured either directly with suitable narrow-band filters (most objects) or inferred from adjacent filters. The spectral region around $12\,\mu$m is free of strong spectral features and thus serves as the best monochromatic estimate of the nuclear MIR continuum luminosity.

The method described in [1] allows for constraining the contribution of SF toward the nuclear $12\,\mu$m emission by using a tight empirical correlation between the strength of the polycyclic aromatic hydrocarbon (PAH) emission feature at $11.3\,\mu$m and the continuum MIR emission in starburst galaxies. PAHs are commonly used as a SF tracer [3]. Therefore, it is possible to scale a SF template spectrum from [2] to the PAH flux in the individual AGN. This PAH flux is in turn either constrained from the lower angular resolution *Spitzer*/IRS spectra of the AGN (if available), or suitable HR photometric covering the $11.3\,\mu$m feature. This method yields an upper limit for the relative nuclear SF contribution at $12\,\mu$m. In the majority of AGN, the maximum SF contribution at sub-arcsec scales is minor. This is particularly the case for type 1 AGN, while type 2 AGN tend to exhibit higher possible SF contribution.

In the following, we present preliminary results for the majority of detected AGN from the AGN MIR atlas. Similar to [4, 7, 1], we have compiled absorption-corrected 2-10 keV X-ray luminosities, $L_{\rm X}$, for most of the detected AGN from the most recent satellite missions and publications. Details and final results for all AGN will be published in Asmus et al., in prep. b.

3.1 Global MIR emission

Whenever the angular resolution is insufficient to separate AGN and host emission, as in particular in higher redshift studies, it is important to assess whether the AGN dominates the observed total MIR emission. For this reason, we compare the HR measurements with low angular resolution measurements from *IRAS*, the beam of which contains most of the host galaxy emission. Fig. 2 demonstrates that the AGN dominates the global MIR emission only at intrinsic X-ray luminosities of $L_{\rm X} \gtrsim 10^{43}$ erg/s although with a large scatter.

3.2 Relation to X-ray emission

The MIR–X-ray correlation has proven to be a powerful tool for AGN studies [10, 4, 12]. For 140 detected AGN of the atlas, we thus compare the X-ray luminosities to the observed monochromatic $12\,\mu$m luminosities, $L_{\rm MIR}$, in Fig. 3. As expected from previous investigations, a strong correlation best described by $\log L_{\rm MIR} = 0.33 \pm 0.03 + (0.99 \pm 0.03) \log L_{\rm X}$ is found. The observed scatter in the MIR-to-X-ray ratio is ~ 0.42 dex, and the intrinsic scatter is estimated to be ~ 0.28 dex with `linmix_err` [9]. The same relation is also present in flux space and therefore is not caused by distance-related effects.

4. Conclusions

We have presented preliminary results for the AGN MIR atlas consisting of 249 local AGN with HR MIR imaging observations with four of the largest optical/infrared telescopes available today. In total, 200 objects have been detected and appear compact in most cases. By comparison

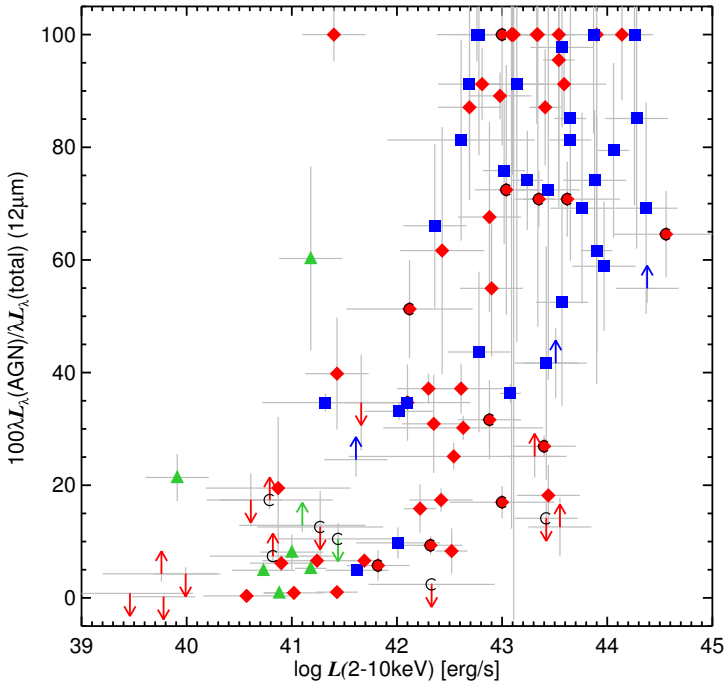

Figure 2: Percentage of the fraction of AGN-to-global MIR luminosity versus the absorption-corrected X-ray luminosities for 140 detected AGN (preliminary). Blue squares: type 1 Seyferts (type 1.5 or lower); red diamonds: type 2 Seyferts; green triangles: LINERs; "C"s mark Compton-thick objects.

with a typical starburst template, we have excluded SF as the main cause of the point-like nuclear emission. Instead, most of the observed MIR emission appears to originate from AGN-heated dust, which still needs further verification. A comparison between high and low angular resolution MIR photometry shows that the AGN dominates the global emission of the galaxies only above AGN luminosities of 10^{43} erg/s. Finally, we find a strong correlation of the observed nuclear MIR emission with the absorption-corrected X-ray emission. Such a correlation can be approximately understood by a link between the MIR and X-ray emission via reprocessing of primary radiation from the accretion disk, which is strongest in the ultraviolet (UV). The latter is reprocessed on the one hand in the innermost regions around the SMBH, where the UV photons are up-scattered from hot corona electrons into the X-ray regime. And on the other hand, much further out in the torus region, the UV photons are absorbed by dust and reemitted as thermal radiation in the MIR. More detailed studies are necessary, however, to test the origin of the MIR emission and its independence from other AGN parameters.

References

[1] D. Asmus et al., *Nuclear mid-infrared properties of nearby low-luminosity AGN*, A&A, 536, 36

[2] B. R. Brandl et al., *The Mid-Infrared Properties of Starburst Galaxies from Spitzer-IRS Spectroscopy*, ApJ, 653, 1129

[3] D. Calzetti et al., *The Calibration of Mid-Infrared Star Formation Rate Indicators*, ApJ, 666, 870

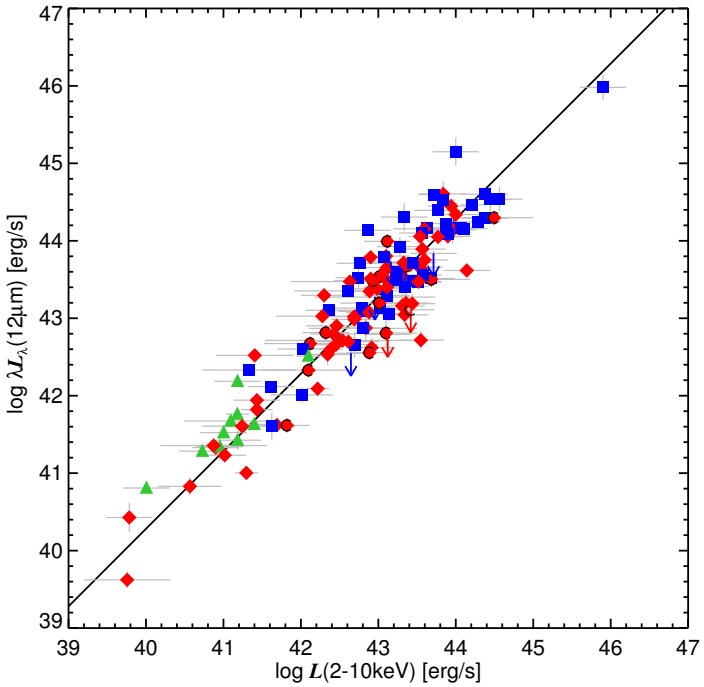

Figure 3: Relation of observed MIR and absorption-corrected X-ray luminosities for 140 detected AGN (preliminary). Symbols are similar to Fig. 2. The line represents the best power-law fit to all data points obtained with `linmix_err`.

[4] P. Gandhi et al., *Resolving the mid-infrared cores of local Seyferts*, A&A, 502, 457

[5] A. C. Glasse et al., *Michelle Midinfrared Spectrometer and Imager*, SPIE, 2871, 1197

[6] V. Gorjian et al. *10 Micron Imaging of Seyfert Galaxies from the 12 Micron Sample*, ApJ, 605, 156

[7] S. F. Hönig et al., *The dusty heart of nearby active galaxies. I. High-spatial resolution mid-IR spectro-photometry of Seyfert galaxies*, A&A, 515, 23

[8] H. Kataza et al., *COMICS: the cooled mid-infrared camera and spectrometer for the Subaru telescope*, SPIE, 4008, 1144

[9] B. C. Kelly, *Some Aspects of Measurement Error in Linear Regression of Astronomical Data*, ApJ, 665, 1489

[10] A. Krabbe et al., *N-Band Imaging of Seyfert Nuclei and the Mid-Infrared-X-Ray Correlation*, ApJ, 557, 626

[11] P. O. Lagage et al., *Successful Commissioning of VISIR: The Mid-Infrared VLT Instrument*, The Messenger, 117, 12

[12] N. A. Levenson et al., *Isotropic Mid-Infrared Emission from the Central 100 pc of Active Galaxies*, ApJ, 703, 390

[13] C. M. Telesco et al., *GatirCam: Gemini mid-infrared imager*, SPIE, 3354, 534

[14] M. Véron-Cetty & P. Véron, A catalogue of quasars and active nuclei: 13th edition, A&A, 518, 10

[15] L. M. Winter et al., *X-Ray Spectral Properties of the BAT AGN Sample*, ApJ, 690, 1322